CLT under in-plane loads: Investigation on stress distribution and creep

Martin Gräfe, Philipp Dietsch and Stefan Winter
Chair for Timber Structures and Building Construction
Technical University of Munich

Keywords: cross-laminated-timber, prestressing, post-tensioning, creep, in-plane behaviour, load distribution, shear

1 Background and objective

Tall buildings need to bear high horizontal loads, particularly from wind and seismic loading. Apart from shear stresses, these loads are generating vertical forces in the bracing elements of such buildings. In steel and concrete structures, vertical tension loads are transferred by reinforcement bars, prestressing tendons, or the steel structure itself. As timber structures feature a comparatively low self-weight to counterbalance vertical tension forces and are typically made up of a relatively large number of single elements, a rather large quantity of fasteners such as screws or dowels is required to transfer the vertical tension forces.

This led to the idea of introducing vertical prestressing elements in order to counterbalance these tension forces. With this system, the horizontal joints only have to bear compression and shear stresses, which are easier to handle and enable the use of e. g. form-fitting connections without additional fasteners.

For the application of this system, it needs to be clear how a concentrated in-plane load introduced by the anchorage of a prestressing tendon into the CLT-panel distributes downwards. In addition, the creep behaviour of CLT loaded under in-plane compression loads is a prerequisite for the application of such systems. The objective of the project described in the following was to contribute answers to these two questions, based on experimental tests and parameter studies.

2 Load distribution in-plane

2.1 Definition of the load distribution angle

A single in-plane load on the narrow edge of an orthotropic plate distributes downwards in a nonlinear manner, governed by several material and geometric parameters. The bearing force on the bottom edge or any horizontal section is distributed in a bell-shaped curve, whose integral over the horizontal length represents the single load applied on the top (Fig. 1 left). For engineering applications (e. g. steel, concrete, masonry) it is widely accepted common practice, to assume a linear distribution over a certain horizontal length, which is normally defined by a fixed angle of load distribution for each material (e. g. 30° for (any type of) masonry, up to 45° for concrete or steel). (Wallner-Novak et al. 2018) recommend an angle of 25° for CLT with 33 % cross-layer proportion, and indicates a range between 15° and 45° between 0 % and 100 % cross-layer proportion.

The approach presented in this paper uses a calculated, respectively measured total width of load distribution (until the strain curve converges to zero), then cuts off 5 % of the integral, and calculates

the angle of load distribution to the point, at which 95 % of the force are covered (Fig. 1 left). The width of the strain distribution was firstly calculated by an FE-parameter study (Westermayr 2016), and subsequently verified by mechanical tests in a specialized test setup.

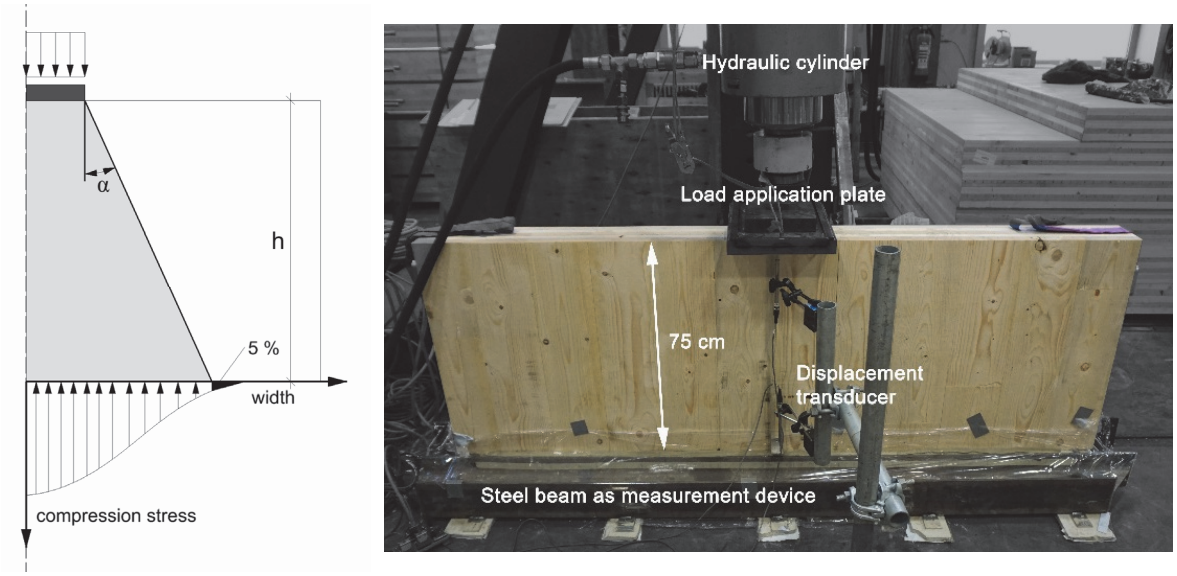

Figure 1 left: definition of the load distribution angle α, right: specimen placed in the test setup

2.2 Parameter Study

A parameter study was realized by means of a FE-model to determine the influence of the parameters on the load distribution angle: narrow face bonding, cross layer proportion, variability of material properties, range of mechanical material parameters, the position of the load application and the height/width proportion of the CLT-element. With the 3-D model, the bearing force of each configuration was calculated and plotted on a diagram over the length of the linear support at the bottom edge. This enabled the calculation of the load distribution angle for each set of parameters.

The model was a volume model representing single boards, which were defined with the material properties shown in table 1. The gaps between single boards were set with a width of 2 mm, the supports were defined as rigid nodal supports, and the FE-mesh featured a squared mesh width of 20 mm (Fig. 2 left). A typical load distribution diagram is shown in Fig. 2 right, similar diagrams where derived for all parameters mentioned above.

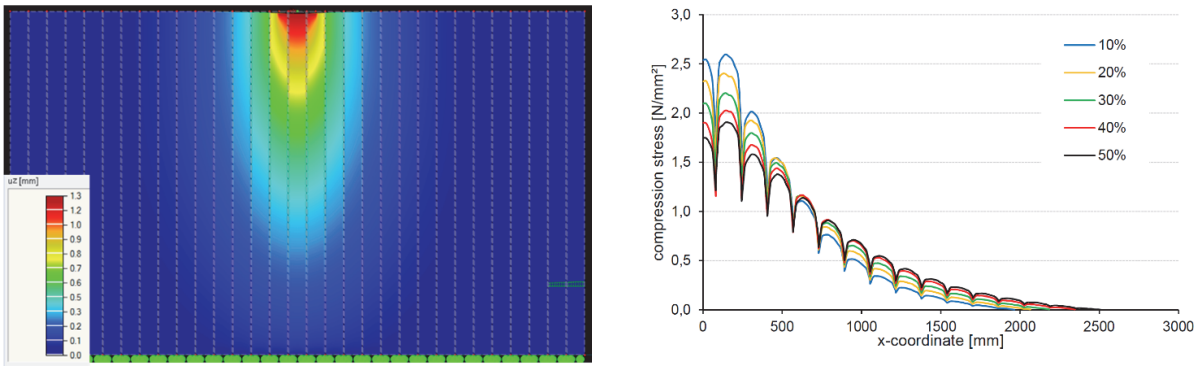

Figure 2 left: FE-model, deformation u_z, right: diagram of load distribution with different cross layer proportions (Westermayr 2016)

Table 1 Material properties for the FE-model, according to (Neuhaus 2009)

E-modulus $[N/mm^2]$			Shear-modulus $[N/mm^2]$			Poisson ratio		
L	R	T	LR	TR	TL	LR	TR	TL
10.000	800	450	600	40	650	0,027	0,6	0,033

The following conclusions from the parameter study can be drawn:

- The cross layer proportion has a significant influence on the width of the load distribution
- Narrow-face bonding leads to a smoother strain distribution, and in total to an increase of the load distribution angle of 2° to 3°
- The poisson ratio and varying material properties show a very low influence
- The wall height in a typical range from 2 m to 5 m has a very small influence
- The board width was 160 mm, broader boards lead to broader load distribution angles, the maximum is identical with the values for narrow face bonded CLT
- The bottom support was ideally rigid. This can never be achieved in practice, leading to broader distributions as calculated.
- The angle of load distribution, taking into account all models and parameters, ranged between 21° (10 % cross layer proportion) and 28 ° (50 % cross layer proportion)

2.3 Experimental investigation

2.3.1 General

To verify and calibrate the results from the FE-model, a series of mechanical tests was conducted. The objective was to measure the force per unit length along the bottom edge of a CLT-plate, which was loaded on the upper edge by a concentrated in-plane load.

2.3.2 Test setup

The measurement of the force per unit length at the bottom of the CLT-panel was done by placing it on a specially designed steel beam, which was equipped with 56 vertically oriented strain gauges. The steel beam was slotted into single elements, featuring 50 mm horizontal length in the middle and 100 mm on the sides of the beam (Fig. 3). The strain gauges provided the vertical compression strain in these elements, which could be converted into compression stress in the steel, correspondingly the force per unit length in the contact line between steel and CLT, and thus the stresses and distribution of stresses in the CLT-element. All strain gauges were calibrated after application to the beam by applying compression strain by calibrated test equipment and verifying the correct readings.

The steel beam was supported sidewise by two steel beams in order to prevent possible lateral deflection, and placed on the concrete floor of the laboratory in a thin layer of high-strength cement grouting to achieve the highest possible vertical stiffness. The joint between steel and CLT was smoothed accordingly with a thin (≈ 1 *mm*) layer of cement grouting, to ensure a full surface contact regardless to minor unevenness.

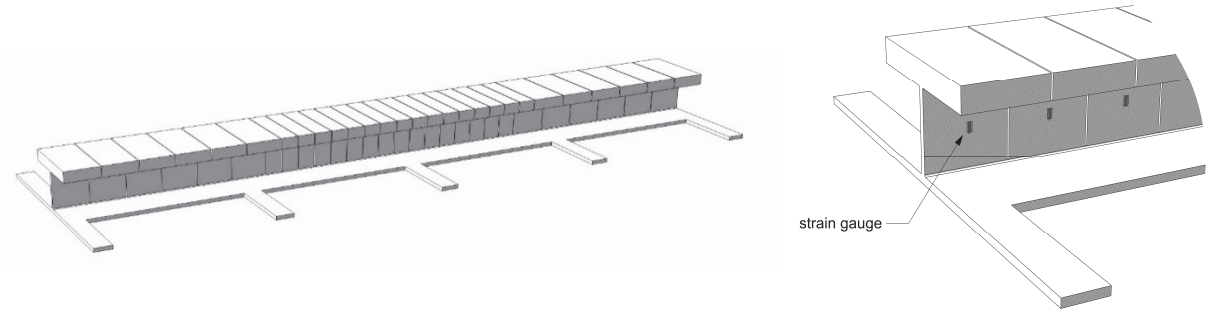

Figure 3 left: steel beam as measurement device, right: detail of single elements with strain gauge

Three different CLT-layups where used, featuring five or seven layers, total thicknesses from 150 to 200 mm, and a proportion of cross layers from 25 % to 40 %. The CLT-elements were not-narrow-face-bonded, graded as C24, and featured a height of 750 respectively 1500 mm, and width of 2000 mm. The load was applied in three steps from 5 N/mm² to 15 N/mm² on the CLT-layers with vertical orientation, by a steel plate of 300 mm length and a force controlled hydraulic cylinder (Fig. 1 right).

2.3.3 Test results

The measured strain and derived mechanical stress distribution showed a bell-shaped curve, as expected with the maximum value in the symmetry line of the load application (Fig. 4 left). This result fitted well with the derived load distribution angle from the results of the FE-model. The strain was plotted over the bottom length, and then a gaussian bell curve fitted to the measurements with the least square method. To this curve the same 95 % rule as used in the FE-study was applied, and the resulting angle calculated. This angle showed a range from 21° at 25 % cross layer proportion, to 23,2° at 40 % cross layer proportion (Fig. 4 right).

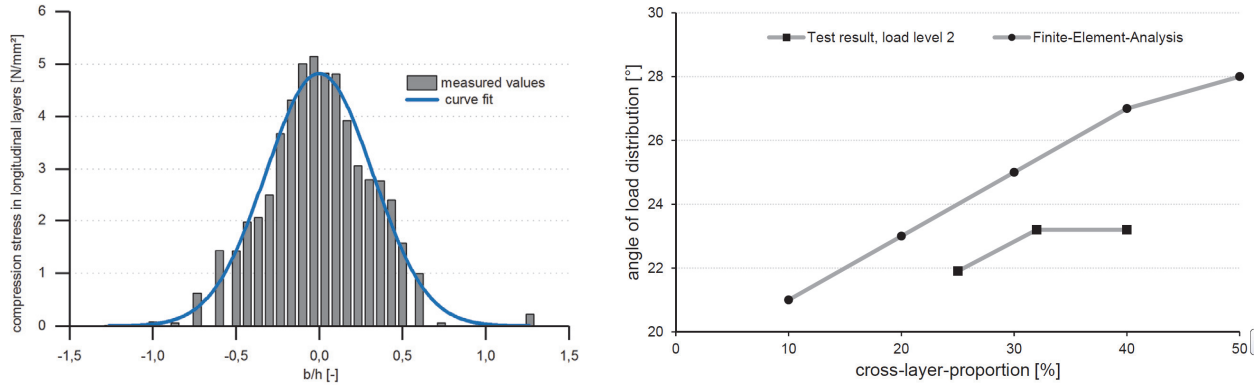

Figure 4 left: measured data and curve fit (40 % cross-layer-proportion), right: comparison between FE-model and test results

2.4 Conclusion

The angle of load distribution in CLT panels is primarily dependent on the bonding of the narrow faces, the width of the single boards, the height of the CLT-element, the proportion of cross layers, the wall height, and the stiffness of the contact surface at the bottom edge. Finite-Element studies as well as mechanical tests showed, that a single load applied on the narrow edge of a CLT panel distributes downwards in an angle of 21° to 28°. For practical engineering use, the assumption of this angle to 25° and a linear strain distribution in any horizontal section appears justified for CLT-walls

up to 5 m height, with or without narrow face bonding, and a cross layer proportion of at least 20 %. This simplified assumption takes into account, that the bottom contact surface in any application of CLT in reality is not “ideally stiff” but always featuring a certain flexibility in z-direction. This leads to a broader distribution of load, and therefore to lower compression stresses as calculated theoretically. Furthermore, the distribution is always nonlinear, with its peak level normally in the centre line under the load application. The approach suggested in this paper uses a linear load distribution, and consequently underestimates the maximum value in the centre. Such an approach is widely used and well established in engineering practice for typical structural materials (masonry, concrete, steel), some of which show typical brittle failure behaviour. The authors consider this approach to be appropriate for CLT as well, bearing in mind its ability for elastic-plastic redistribution of loads to lower stressed regions within the panel under in-plane loads. In addition, the verification against buckling of 2-dimensional CLT panels is typically on the safe side when it is realized as uniaxial verification on a “representative 1-m-strip” e. g. with the equivalent member method.

Regarding the question of standardisation it may be taken into account that practice asks for calculation methods as manageable, less error-prone and less time-consuming as possible. More detailed approaches may be more accurate in some cases, but tendency for misinterpretation or disapproval of practice is higher due to reasons of time and qualification of engineers.

3 Creep behaviour of CLT under compression stresses in plane

3.1 Influencing factors

The creep behaviour of timber is mainly dependent on the type of mechanical stresses (bending, shear, tension, compression), size, type and grade of specimens, moisture content and changes in moisture content and load level. In particular the ambient conditions and resulting changes in timber moisture content contribute a large share to the long-term behaviour, generally intensified with reduction of size of specimens. The type of processing, respectively the type of the final timber product is relevant as well, as influences like grading, cut type, thickness of lamellas and added glue may add additional uncertainty and statistic scatter to any mathematical prediction of the creep behaviour. Due to this broad range of parameters, tests results and – to an even higher extent – extrapolated final creep ratios found in literature show an extensive variety.

3.2 Literature und existing test results

Most creep tests described in literature where realized as bending tests in different setups, often with rather small specimens and in some cases from ungraded timber.

Literature on creep tests can be roughly divided into two areas of interest: The first group is represented by the creep behaviour of bending beams, which are loaded by quasi-permanent loads perpendicular to the longitudinal axis. Depending on the geometry, different proportions of tension, compression and shear stresses result in this type of specimen, and lead to corresponding creep behaviour. Consequently, deflections perpendicular to the longitudinal axis where measured over time (e. g. (Gressel 1983), (Rautenstrauch 1989), (Jöbstl et al. 2007)). The second group is represented by creep and load carrying capacity tests with slender compression members. This research intended to investigate, describe and predict the long-term-load capacity in terms of a possible stability failure due to increasing strain induced by second order effects. Usually, the specimens where loaded with

combined compression and bending strain, and different imperfections where applied. The measured parameter was normally the deflection perpendicular to the member's axis, similarly to the method known from bending tests. ((Härtel 2000), (Becker 2002), (Hartnack 2004), (Morlier 2007), (Moorkamp et al. 2001))

Unfortunately, especially in older literature, the load levels were often not specified. This makes it difficult to compare tests results, and to draw conclusions on the behaviour of real-size CLT from graded and kiln-dried boards loaded in compression. Some scientific evidence (Glos et al. 1987), (Blaß 1988) suggests, that creep test results from bending, or combined bending and compression may not fit to the creep behaviour of timber under pure compression load. For a realistic design of prestressed timber members, the creep behaviour in longitudinal direction is the only relevant parameter for the prediction of losses in prestressing force. The question of stability, or respectively long term load carrying capacity is to be answered in an additional second step, by using creep values derived from bending tests as mentioned above.

On this basis, a specific series of creep tests in different load grades and climate conditions was realized, to get more specific results for the application "CLT under longitudinal compression".

3.3 Experimental test setup

3.3.1 General layout

The test series consisted of seven creep tests, with three different load levels and three different climate conditions (Table 2). All test specimens where made of 5-layered CLT, without edge bonding, featuring a length of 8,0 m and a width of 150 mm (Fig. 5 and Fig. 6). The CLT was made of spruce, graded as CL24, and retrieved from the normal production line of Züblin Timber GmbH in Aichach, Germany. The average density was 440 kg/m^3, the timber moisture content was u = 10,8 %. No abnormal visual characteristics or damages were observed, the precision of machining, gluing and straightness was as planned and ordered.

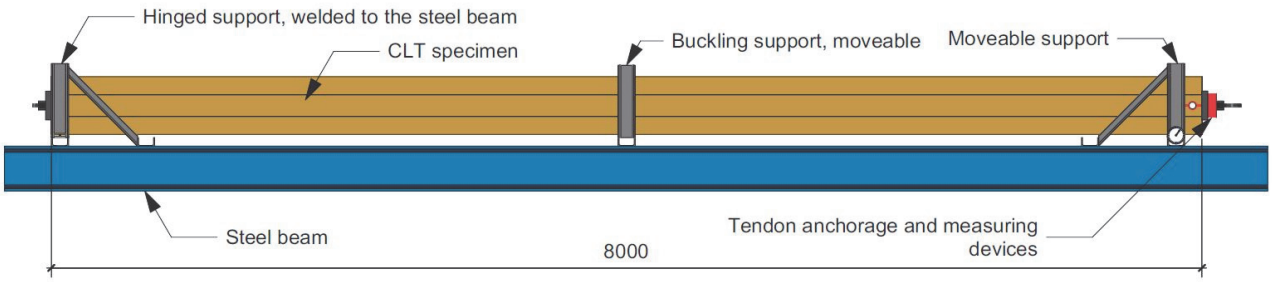

Figure 5 General layout of the test setup

The compression stress applied to the longitudinal lamellas was 5, 10 and 15 N/mm². The compression force was applied by a single unbonded monostrand tendon St 1660/1860, A_P = 150 mm², which was inserted in a centric slot of 34 x 34 mm² (Fig. 6 left). This slot was applied during production of the panels by adding and later removing corresponding spacers. This method is described in detail in (Gräfe et al. 2018). The specimens were placed in pairs on a steel beam, which was equipped with welded-on hinged and moveable supports. One side of each specimen was fixed against the steel beam, while the other end was able to move freely in longitudinal direction. The moveability of the supports was ensured by roller bearings, and partly PTFE-sheating between timber and steel. This setup ensured that the steel beam was free of any force resulting from deformations of the timber,

and that the measured force was completely transferred by the corresponding specimen. The distances of the lateral supports were calculated as to prevent buckling in any direction, and were set to 4,0 m for the specimens type A, and 2,0 *m* for the specimens type B and C (Fig. 5 and 6 left).

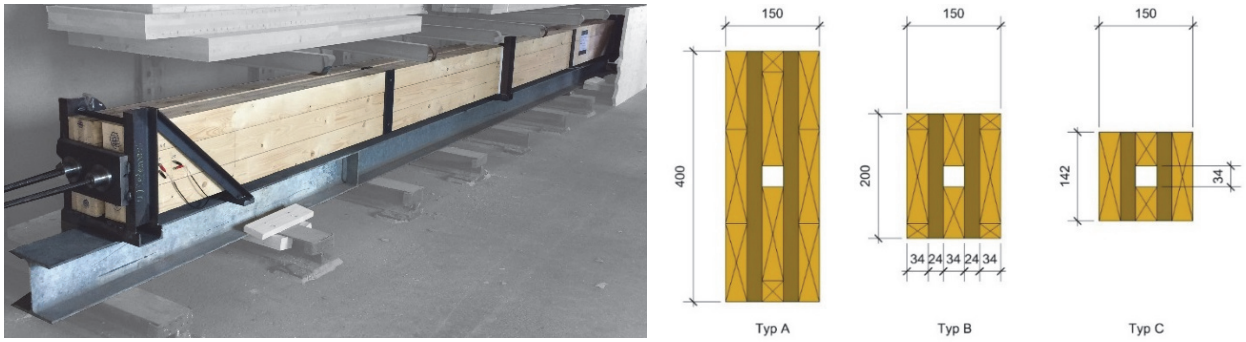

Figure 6 left: view of specimen B2 and C2 at the outdoor test location, right: cross sections of test types A, B, C

3.3.2 Prestressing process

Each tendon, resp. specimen, was prestressed to approximately 220 *kN* by a hand-driven hydraulic jack. After the wedges were driven into their seats and the hydraulic pressure released, the force dropped to the $P_{m,0}$ value, which was between 203 *kN* and 210 *kN.* During the prestressing process the deformations and forces where measured, allowing to subsequently calculating the individual modulus of elasticity of each specimen (Table 2).

Table 2 Specimen properties, prestressing forces, deformations and calculated modules of elasticity

Test No.	A1.1	A1.2	B1	B2	C1	C2	C3
P_{max} $[kN]$	220,0	221,0	222,0	221,5	222,9	220,5	222,5
$P_{m,0}$ $[kN]$	203,7	206,5	207,7	209,5	210,3	208,2	210,5
u_0 $[mm]$ @ $P_{m,0}$	4,40	3,76	7,65	7,40	9,91	10,10	11,02
E $[N/mm^2]$	9.379	11.083	11.292	12.738	12.738	11.466	11.466
σ_c $[N/mm^2]$	5,0	5,0	10,0	10,0	15,0	15,0	15,0
A_{net} $[mm^2]$	39.644	39.644	19.244	19.244	13.328	13.328	13.328
$\sigma_c/f_{c,0,mean}$ $[\%]$	14	14	28	28	42	42	42
Climate type (see. 3.4)	1	1	1	2	1 + 3	2	3
Duration $[h]$	1.400	1.400	2.000	9.800	9.800	9.800	7.300

3.3.3 Measuring systems – force, ambient conditions, deformation

In climate 2, the measurements of tendon force, ambient conditions, the material temperatures of the CLT specimen and the supporting steel beam and deformation of the specimens were realized electronically by means of load cells (500 *kN* Type 722, Induk GmbH), relative humidity and air temperature sensors from the modularized programmable e *Tinkerforge* System, and inductive displacement sensors. The deformation of the specimens in climate 1 and 3 (laboratory at TUM) was measured by mechanical gauges (Fig. 7). Both the inductive sensors and mechanical gauges had an accuracy of 1/100 *mm*, while the load cell had a guaranteed accuracy of ± 1 %.

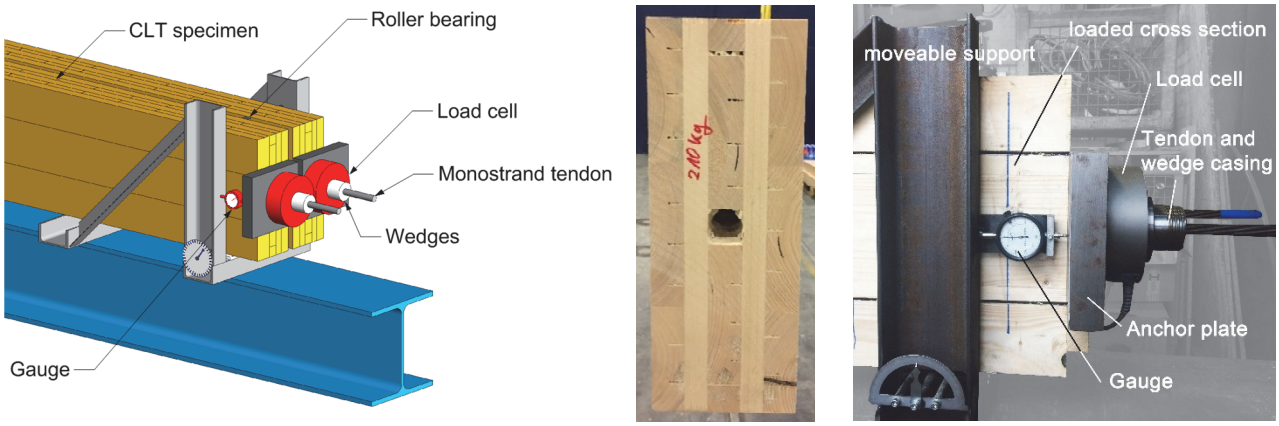

Figure 7 left: detail drawing of measuring devices, middle: cross section type A, right: side view of measuring devices

3.3.4 Measuring systems – timber moisture content

The timber moisture content for the specimens in climate 1 and 3 was measured continuously with the electric resistance method and permanently installed electrodes. The applied method and technical equipment was identical with the systems described in (Dietsch et al. 2015). (Mugrauer GmbH, Gigamodul and Softfox software). Eight pairs of electrodes where applied in depths from 15 *mm*, 25 *mm*, 40 *mm* and 70 *mm* at representative locations throughout the specimens. Representative timber moisture contents are plotted over time in fig. 9 left.

The timber moisture content of specimen B2 and C2 in the outdoor test in Aichach was measured at least every four weeks by a hand-held electric resistance-type measuring device (Type GANN Hydromette RTU 600), at eight permanently installed pairs of electrodes in 15 *mm* and 25 *mm* depth.

3.4 Ambient climate conditions

3.4.1 Types of climate

Three different climate conditions where used: a constant climate of 20° C and 60 % RH (Climate 1), the natural outdoor climate in Aichach, southern Germany (Climate 2), and a climate cycle with weekly changes between 40 % and 90 % RH (Climate 3).

3.4.2 Climate 1

The tests were performed in the timber test laboratories of TUM, in which relatively constant ambient conditions are ensured by a heating and air moisturising system. Slight variations in the climate conditions typically occur by the occasional opening of windows and entrance gates, and by the influence of the outdoor air temperature in summer as no cooling system is installed.

3.4.3 Climate 2

The location was a rain-sheltered, shady place in an all-side open storage shed in Aichach, Germany (48°26'29.2"N 11°07'11.0"E, fig. 6 left). The described test period lasted from May 2017 to June 2018, the climate was typical for the region of southern Germany. The measured relative humidity and temperature is shown together with the Savitzky-Golay-filtered data in fig. 8. The filtered relative humidity ranged from approximately 60 % RH to 90 % RH, while the according temperature range was – 3 °C to 22 °C (Fig. 8).

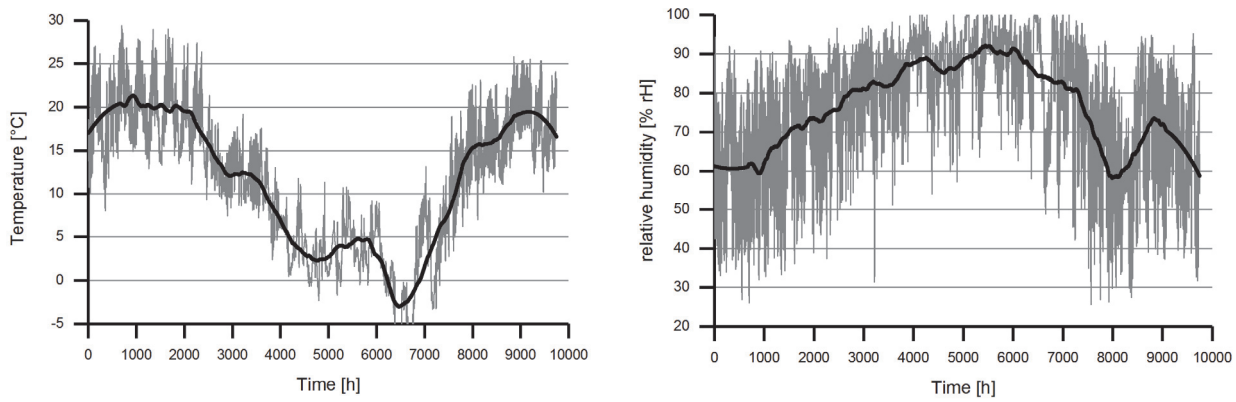

Figure 8 Air temperature (left) and relative humidity (right) in Aichach, Germany from May 2017 to May 2018 (Climate 2)

3.4.4 Climate 3

After the tests in constant climate 1 conditions where finished, the test setup in the laboratory was encased with plastic sheeting, followed by the placement of a customary ultrasonic air humidifier and a condensation dryer inside. This machinery was fitted with integrated sensors and controllers, which kept the conditions automatically at the preselected values. The volume of the casing was approximately 10 m³, which was constantly circulated by an electric fan with a capacity of 125 m³/h to ensure even conditions within the whole volume. As the temperature in the laboratory was conditioned to a relatively constant level, the temperature in the test casing remained constant as well at any humidity conditions inside. The climate cycles consisted of four dry (40 % RH) and four wet (90 % RH) 7-day phases, followed by a four-week wet, and a five week dry phase. The measured relative humidity over time is shown in fig. 9 left, together with the intended nominal values. Before and after the cyclic changes the conditions were constant as described for climate 1. Some scattering occurred around 2.000 *h* due to testing procedures of the air conditioning machinery.

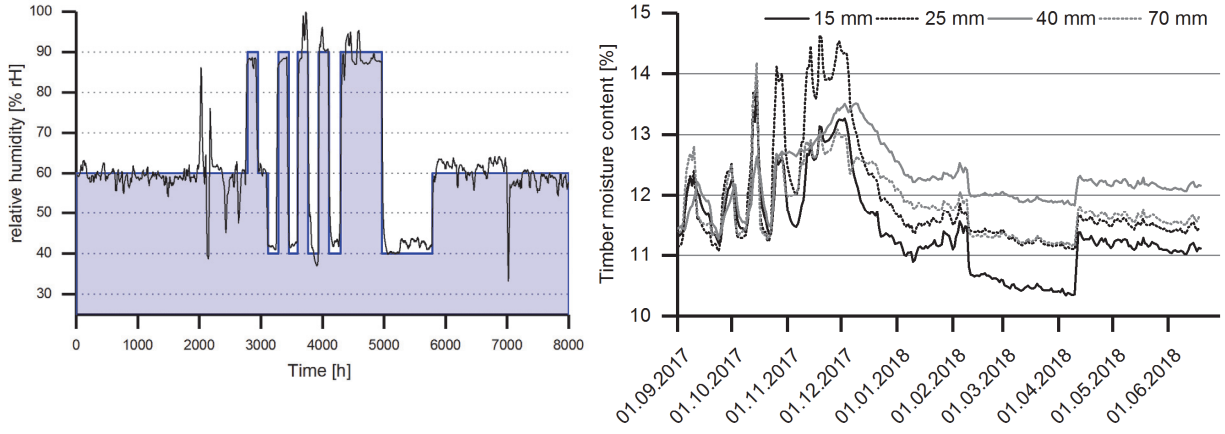

Figure 9 Relative humidity (left) and measured timber moisture content (right) in climate 3

3.5 Modelling of creep deformations

3.5.1 Calculation method for creep deformations

The reading of the gauges, respectively of the inductive deformation sensors show the superposition of influences from creep, shrinkage, swelling, variations in tendon force and temperature. To derive the desired creep deformation, the gauge reading has to be corrected by these parameters. As influences from changing timber moisture content are difficult to describe and to calculate, only time periods with identical timber moisture contents were investigated for the creep evaluation.

The tendon force was measured over time. In combination with the known individual modulus of elasticity, this allowed easily to account for varying deformation due to variations of compression force, respectively compression strain in the CLT elements.

Temperature changes were taken into account by using the measured material temperatures, and assuming thermal expansion coefficients of 6,0 * 10^{-6} for timber longitudinally and of 12,0 * 10^{-6} for steel. All deformation plots and derived creep values presented hereinafter are correspondingly corrected values according to the following formula:

$$u_{creep} = u_{measured} + u_{T,steel} + u_{T,timber} + u_{\Delta P} + u_{S+S}$$

3.5.2 Creep model and extrapolation

The test results in this research project were analysed and extrapolated by the rheological model introduced by (Pfefferle 1971), see fig. 10. This model consists of two springs, and one non-linear damper. The model was introduced originally to describe the behaviour of concrete, adapted to timber by changing the linear to a non-linear damper by (Rheinhardt 1973), and evaluated by test results from (Möhler and Maier 1970) and (Kollmann 1964). The model is equivalent to the standard solid model, but uses a damping element whose force is proportional to the square root of the time. The element deforms faster in the beginning, but converges significantly slower to its final value compared to the standard solid model.

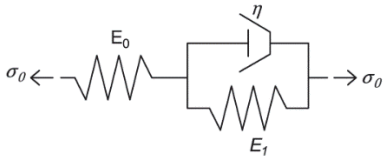

$$\varepsilon(t) = \frac{\sigma_0}{E_0} + \frac{\sigma_0}{E_1} \cdot \left(1 - e^{-\frac{E_1}{\eta} \cdot \sqrt{t}}\right)$$

Figure 10 left: Rheological model from Pfefferle, right: formula

Advantages of this model are its good fit to the natural behaviour of wood, and the relatively simple interpretability. More complex models which integrate directly e. g. the mechano-sorptive effects (Hanhijärvi 1995), (Toratti 1992) provide theoretically a better fit to test results, with the difficulty to correctly determine the necessary parameters, which are mutually dependent in a rather complex, highly nonlinear manner. Although even simpler models such as the exponential model (used e. g. by (Wanninger 2015)) may provide a good fit to the initial time of a creep test, they seem to be less adequate to correctly approximate the behaviour over longer periods.

After extensive literature review the *Pfefferle*-model was chosen from as the best compromise between a good fit to natural material behaviour, and simplicity und comprehensibility of its parameters.

3.6 Results

3.6.1 General observations

The tendon forces decreased only slightly (less than 5 %) over time, mostly due to relaxation of the tendons. This is understandable, as the lengthening of the tendons during initial prestressing was about 100 *mm*, while the creep deformations of the timber reached only to 3 *mm* in the maximum. No buckling or visible lateral deflections were observed.

The reaction of the specimens to changes in relative humidity was very sensitive. For instance a temporary opening of windows with a resulting drop in relative humidity of up to 10 % led to a clear reaction to the length of the specimen of some 1/100 *mm* within approximately half an hour.

Shrinkage due to drying of the timber has a strong impact on total deformation, while swelling due to moisturizing in the same extent leads to lower values. All changes in timber moisture content lead to a clear increase of creep deformation.

3.6.2 Tendon force

The losses in tendon force fit well to the calculated values derived from the technical approval (Z-12.3-84) of the used monostrand tendons St 1660/1860 with *very low relaxation* (Fig. 11). Therefore the calculation approach stated in the approval was subsequently used to determine relaxation losses.

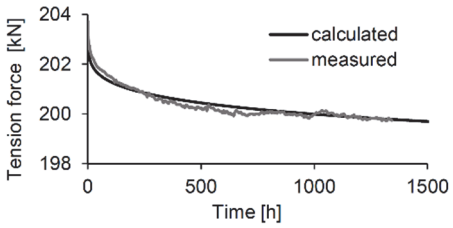

Figure 11 Measured and calculated values of tendon force, Test A1.1

3.6.3 Tests in indoor climate, specimens A1, B1, C1

The test results of the specimen A1, B1, C1 together with the related creep model curves are shown in fig. 12. Clearly visible is a better fit and clearer creep curve, as higher the load level is. Test A showed a considerable scatter and no clear measurements, as the influence of interferences like slight changes in temperature or relative humidity is relatively high. Specimen B1 and C1 show a pretty good fit to the selected creep model, and a clear decrease in the speed of creep deformations. The creep ratios were approximately 0,06 after 2000 h for specimen B1, and 0,10 for C1 respectively.

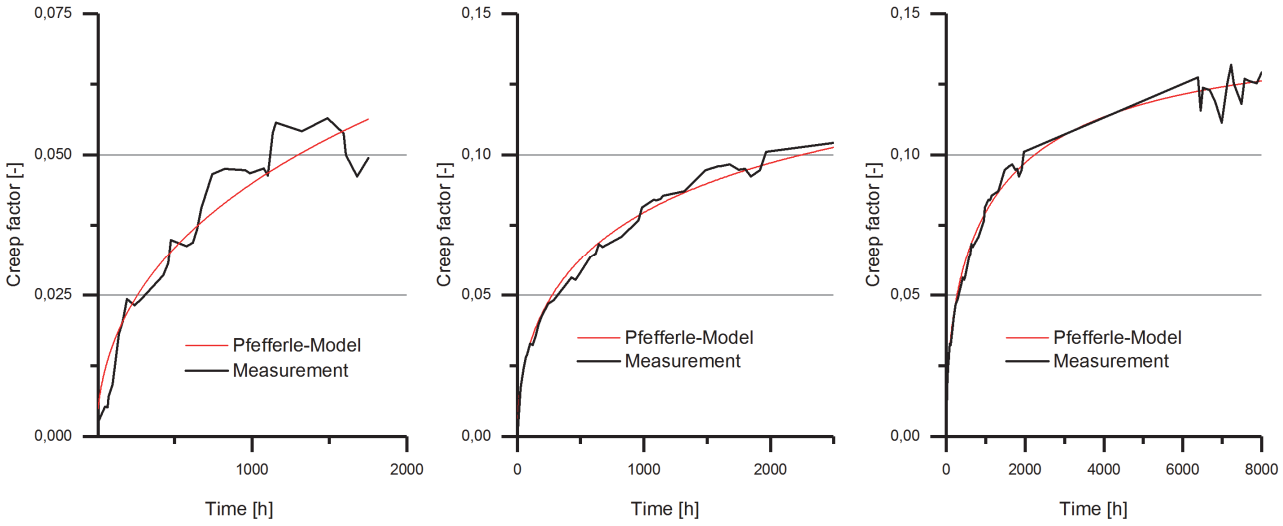

Figure 12 Creep test results and Pfefferle-models for constant climate, from left to right Tests B1, C1 to 2500 h, C1 to 8000 h

The parameters for the *Pfefferle*-models of specimen B1 and C1 were determined as follows:

$$\varphi_{B1}(t) = 0{,}15 \cdot \left(1 - e^{-0{,}01125 \cdot \sqrt{t}}\right)$$

$$\varphi_{C1}(t) = 0{,}2 \cdot \left(1 - e^{-0{,}01652 \cdot \sqrt{t}}\right)$$

For specimen A1 no parameters were calculated, as the measurements were not sufficiently stable and generally very low.

3.6.4 Tests in cyclic climate, specimens C1 and C3

The measured deformation of specimen C1 is plotted together with the nominal relative humidity in fig. 13 left. The strong dependency of deformations on the relative humidity – and according timber moisture content– is clearly visible. Specimen C3 followed the behaviour of C1 very closely, although it was loaded initially at the beginning of the cyclic climate change at around 2500 *h*.

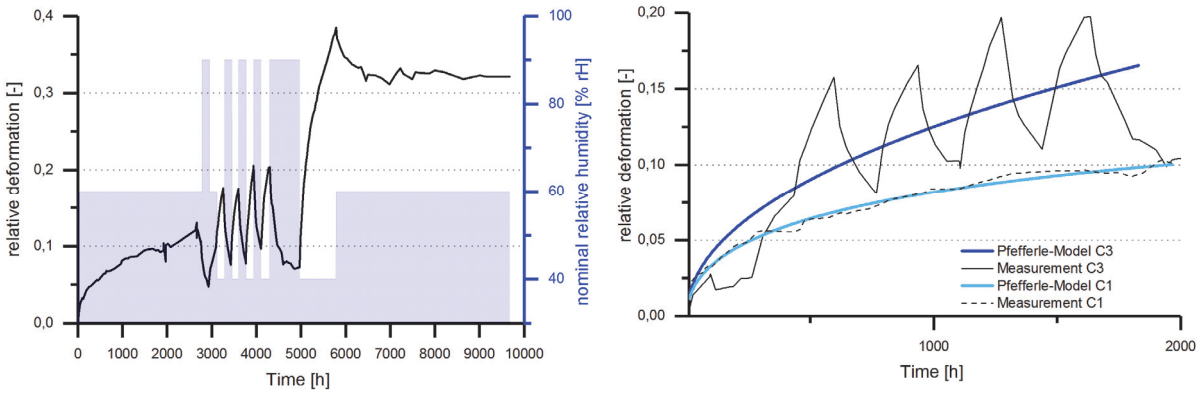

Figure 13 left: Measured deformation and nominal relative humidity of C1, right: comparison of the deformations of C1 and C3

The creep deformations in the cyclic climate are approximately twice as high as in constant climate (Fig. 13 right). Interestingly, the creep deformation does not increase further after ≈ 6000 *h*, which supports the assumption of the existence of a final creep ratio (Fig. 13 left). The parameters for the *Pfefferle*-model of specimen C3 were determined as follows:

$$\varphi_{C3}(t) = 0{,}4 \cdot \left(1 - e^{-0{,}01193 \cdot \sqrt{t}}\right)$$

3.6.5 Tests in natural outdoor climate, specimens B2 and C2

The relative deformation of specimens B2 and C2 is shown in fig. 14 left as smoothed and temperature- and force-corrected (see section 3.5.1) measurement data. The grey line comparatively represents the *Pfefferle*-model of specimen C3 (section 3.6.4), which is considered to be representative for service class 2 conditions. Remarkable is the strong dependency of deformation to relative (air) humidity. The relative deformation grew with its maximum speed by about 0,2 in 1000 *h*. In the timespan up to approximately 7000 *h* (March 2018), the creep deformation is superimposed by the lengthening of the specimen due to swelling, resulting in *negative* relative deformations. As the relative humidity decreased substantially starting in March 2018, the timber moisture content followed accordingly (Fig. 14 right). As the test was started in March 2017, the moisture content of both specimen was on average u = 10,8 % and increased subsequently to its maximum of u = 15,6 % in December 2017. Until summer 2018 the specimen dried to a moisture content of u = 12 %. As swelling is partly impeded by the compression stress of the prestressing, the *lower* compression strain of specimen B2 resulted in *larger* swelling effects compared to specimen C3. Both tests B2 and C2 deformed to a lesser extent as the model C3 (grey curve) suggests.

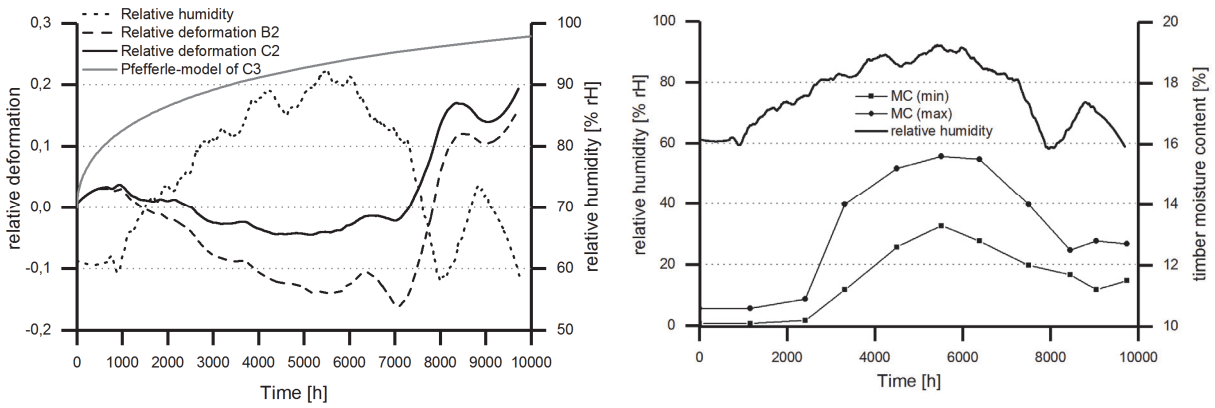

Figure 14 left: relative deformations of specimen B2 and C2, plotted together with relative humidity over time, right: dependency of relative humidity and timber moisture content

3.6.6 Extrapolated final creep ratios

Recommendations for final creep ratios derived from the creep models are shown in table 3. They represent the expected relative creep deformation after an assumed timespan of 500.000 *h*, which is about 57 years.

Table 3 Final creep ratios derived from the Pfefferle-model after 500.000 h, CLT from spruce loaded by compression in grain direction

Load level $\sigma_c/f_{c,0,mean}$	SC 1	SC 2
over 30 %	0,2	0,4
from 15 % to 30 %	0,15	0,3
under 15 %	0,1	0,2

3.7 Conclusion

All test results show creep deformations which are significantly lower than expected from literature data and design standards (e. g. (*Gressel* 1983) and (Eurocode 5)). This applies to the comparison of measured data at any specific time, as well as to final creep ratios derived from extrapolations with the applied creep model.

The difference between test results and literature can be explained by the different test setup and boundary conditions. Most tests reported in literature were conducted as bending tests either with small clear specimen, or solid wood. In the present test series, real-size CLT-specimen made from graded, kiln-dried, finger jointed sawn timber were used and stressed by compression in grain direction at specified practical load levels. *Glos et al.* (1987) report similar results from tests with specimens under compression stress. Based on this data *Blaß* (1988) recommends a final creep ratio of 0,1 for compression stress at constant climate, and twice this value (0,2) for changing climate conditions as typical in SC 2. This approach can be confirmed by the comparison between tests C1 and C3, where the changing conditions lead to a doubling of the creep deformations (Fig. 13 right). The tests in outdoor climate show a strong dependency of deformations on the variation of relative humidity over the course of the year. Anyway, the overall creep deformations in the natural climate do not exceed the deformations realized in the artificial climate with weekly cycles in climate type 3.

The test results lead to the first recommendation, that creep tests on timber should be conducted always with boundary conditions similar to the intended practical application (size and type of specimen, load level, direction of strain, climate conditions, moisture content and grading). Any setup

using test specimen and boundary conditions with properties diverging significantly from the intended application will result in measurements which are difficult to transfer into practice. Although improvements have been made in the last years in the field of computational creep modelling, related results are still associated with significant uncertainties.

Secondly, the conclusion may be drawn that current creep values stated in (Eurocode 5) significantly overestimate the creep behaviour of CLT or glulam under compression stresses in grain direction, especially for service class 1 conditions and stresses below 15 N/mm². The test results do not confirm the assumption that bending and compression creep has more or less the same level, instead compression creep seems to be significantly lower.

Following this, for the design of prestressed timber elements primarily loaded in grain direction it is proposed to answer the following two questions separately: The design regarding *bending* effects (including buckling and other stability cases) should be performed using creep factors derived from *bending tests*, the known data from standards and literature may apply. The calculation of *prestressing losses* is a question of creep due to *compression in grain direction*, and accordingly a shortening of the element. Consequently, creep factors derived from *compression* tests will result in correct calculation results. As only few references provide such test data, results from (Glos et al. 1987) and additionally this publication may be used.

4 References

Becker, P. (2002) *Modellierung des zeit- und feuchteabhängigen Materialverhaltens zur Untersuchung des Langzeittragverhaltens von Druckstäben aus Holz,* Dissertation, Bauhaus Universität Weimar, Shaker Verlag, Aachen

Blaß, H.-J. (1988) *Einfluss des Kriechens auf die Tragfähigkeit von Holzdruckstäben,* Holz als Roh-und Werkstoff 46 S. 405-411, DOI 10.1007/BF02608201

Eurocode 5 (2010) *Design of timber structures - Part 1-1: General and rules for buildings.* CEN. (EN 1995-1-1).

Glos, P., Heimeshoff, B., Kelletshofer, W. (1987), *Einfluss der Belastungsdauer auf die Zug- und Druckfestigkeit von Fichten-Brettlamellen* Holz als Roh-und Werkstoff 45, p. 243-249, DOI 10.1007/BF02616418

Dietsch, P., Gamper, A., Merk, M., Winter, S. (2015) *Monitoring building climate and timber moisture gradient in large-span timber structures* Journal of Civil Structural Health Monitoring, Vol. 5, No. 2, DOI 10.1007/s13349-014-0083-6

Gräfe, M., Dietsch, P., Hipper, A., Wild, M., Winter, S. (2018) *Vorspannung von Brettsperrholzkonstruktionen*, Abschlussbericht, Technical University of Munich, Chair for Timber Structures and Building Construction, München

Gressel, P. (1983) *Rheologisches Verhalten von Holz und Holzwerkstoffen* Abschlussbericht, Versuchsanstalt für Stahl, Holz und Steine, Karlsruhe

Hanhijärvi, A. (1995) *Modelling of creep deformation mechanisms in wood,* Dissertation, Helsinki University of Technology, Technical Research Centre of Finland, Helsinki

Härtel, J. (2000) *Experimentelle und theoretische Untersuchungen zum Kriechverhalten hölzerner Druckstäbe unter baupraktischen Bedingungen,* Fortschritt-Berichte VDI Reihe 4, Bauingenieurwesen, Vol. 159, VDI-Verlag, Düsseldorf

Hartnack, R. (2004) *Langzeittragverhalten von druckbeanspruchten Bauteilen aus Holz,* Dissertation, Bauhaus-Universität Weimar, Weimar

Jöbstl, R., Schickhofer, G. (2007) *Comparative Examiantion of Creep of GLT- and CLT-Slabs in Bending,* Paper 40-12-3, CIB-W18, Meeting 40, Bled, Slovenia

Kollmann, F. (1964) *Über die Beziehungen zwischen rheologischen und Sorptions-Eigenschaften (am Beispiel von Holz),* Rheologica Acta 3, Nr. 4, p. 260–270

Möhler, K., Maier, G. (1970) *Kriech- und Relaxations-Verhalten von lufttrockenem und nassem Fichtenholz bei Querdruckbeanspruchung.* European Journal of Wood and Wood Products 28, No. 1, p. 14–20, ISSN 0018-3768

Morlier, P. (2007) *(Ed.) Creep in Timber Structures.* Taylor & Francis, New York

Moorkamp, W.; Becker, P.; Schelling, W.; Rautenstrauch, K. (2001) *Long-term experiments with columns: Results and possible consequences on design*. Paper 34-2-1, CIB-W18, Meeting 34, Venice, Italy

Neuhaus, H. (2009) *Ingenieurholzbau: Grundlagen - Bemessung - Nachweise – Beispiele.* 2. Ed., Vieweg + Teubner, Wiesbaden

Pfefferle, R. (1971) *Zur Theorie des Betonkriechens,* Dissertation, Technische Hochschule Karlsruhe, Karlsruhe

Rautenstrauch, K. (1989) *Untersuchungen zur Beurteilung des Kriechverhaltens von Holzbiegeträgern,* Dissertation, Universität Hannover, Hannover

Reinhardt, H.-W. (1973) *Zur Beschreibung des rheologischen Verhaltens von Holz*, Holz als Roh- und Werkstoff 31 p. 352–355. – ISSN 0018-3768

Toratti, T. (1992) *Creep of timber beams in a variable environment,* Dissertation, Helsinki University of Technology, Technical Research Centre of Finland, Espoo

Wallner-Novak, M.; Augustin, M.; Koppelhuber, J.; Pock, K. (2018) *Brettsperrholz Bemessung: Anwendungsfälle* proHolz Austria, Wien

Westermayr, M. (2016) *Mechanical behaviour of CLT under concentrated loads in-plane: A finite element analysis,* Master's Thesis, Technical University of Munich, Chair for Timber Structures and Building Construction, München

Discussion

The paper was presented by M Gräfe

H Blass commented that the steel tendon is used to pre-stress and creep is defined as deformation under continuous load. He questioned whether the loading can be considered continuous. M Gräfe agreed that they do not have continuous loading.

S Aicher discussed the use of steel supporting rail and asked how the buckling load was determined under such loading condition. M Gräfe responded that an average load at mid height was used.

H Blass and M Gräfe discussed the meaning of buckling of the CLT whether it is bending stiffness based or compression failure based.

S Aicher asked which width of the load distribution is considered. M Gräfe answered that it is the load corresponding to the width at mid height of the CLT panel. He also said that some FEM studies on 2D elements has been performed which show high capacity compared to individual columns.

A Frangi asked what happens when the load is not applied at the middle. M Gräfe said that the situation is not the same and will be different. He said that it will be a good future topic. A Frangi received confirmation that the beams were end sealed.

H Blass asked about the effective width for buckling design. M Gräfe explained that it is based on the load distribution angle to establish the width at mid height. H Blass said that if you have continuous load versus concentrated load and you cut out a strip, it would be too conservative. You could use a large effective width from the remaining part of the member which takes some loads.

U Kuhlmann commented that the load distribution needs to be examined carefully. There is a big different between parallel to face grain and perpendicular to face grain loading and the angle should be bounded to stiffness. M Gräfe responded that this is already considered based on the percentage of cross layers in the panel.

I Abeysekera asked how conservative is the proposed method compared to the length of effective width approach. I Abeysekera and M Gräfe discussed about the load distribution angle always between 20 to 30 degrees.